Wave modelling in a cylindrical non-uniform helicon discharge

L. Chang[1], M. J. Hole[1], J. F. Caneses[1], G. Chen[2], B. D. Blackwell[1], C. S. Corr[1]

[1] *Plasma Research Laboratory, Research School of Physics and Engineering, Australian National University, Canberra, ACT 0200, Australia*

[2] *Oak Ridge National Laboratory, Oak Ridge, Tennessee 37831, USA*

Abstract

A radio frequency (RF) field solver based on Maxwell's equations and a cold plasma dielectric tensor is employed to describe wave phenomena observed in a cylindrical non-uniform helicon discharge.

Experimental setup

Figure 1 shows a schematic of MAGPIE (MAGnetized Plasma Interection Experiment) and introduces a cylindrical (r, θ, z) coordinate system.[1] For the present study, an RF power of 2.1 kW and 13.56 MHz, and an antenna current of magnitude $I_a = 38.8$ A are used. Argon gas is used with a filling pressure of $P_B = 0.41$ Pa.

Plasma profile diagnostics

A passively compensated Langmuir probe was employed in our experiment to measure the plasma density and electron temperature. Typical measured axial profile of field strength and radial profiles of plasma density and electron temperature in MAGPIE are shown in Fig. 2.

Wave field diagnostics

Helicon wave fields were measured by a 2-axis "B dot" or Mirnov probe. To measure the axial profiles of B_r and B_z, the probe was inserted on axis from the end of the target chamber,

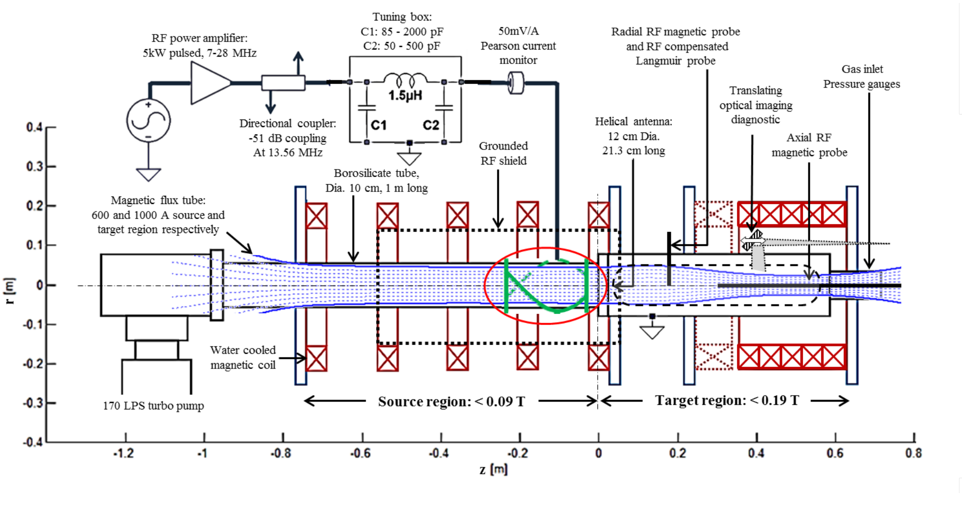

Figure 1: A schematic of the MAGPIE, with left hand half-turn helical antenna.[1]

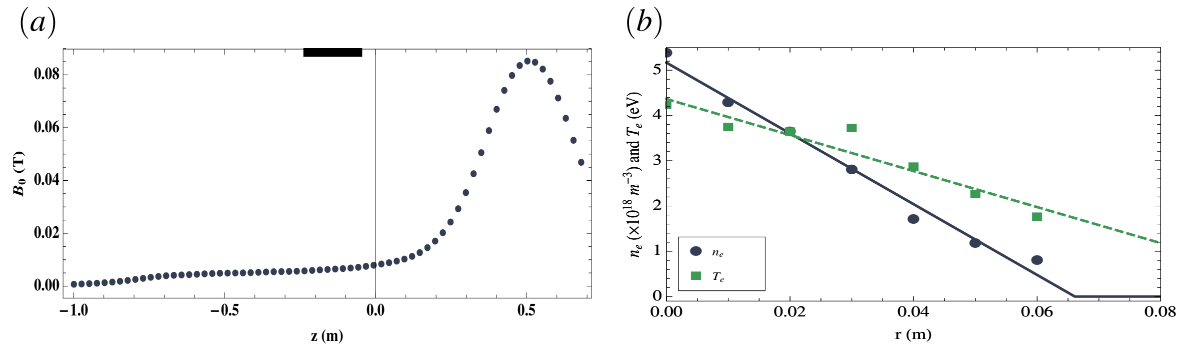

Figure 2: Typical measured profiles: (a) axial profile of static magnetic field on axis, (b) radial profiles of plasma density (dots) and electron temperature (squares) at $z = 0.17$ m, together with the fitted lines. The solid bar in (a) denotes the antenna location.

and to measure the radial profiles of B_r, B_θ and B_z, the probe was inserted radially at $z = 0.17$ m and rotated about its axis. Both axial and radial profiles of wave phase were measured through a phase-comparison method, compared with the phase of antenna current.

Theoretical model

Details of the RF field solver can be found in Chen et al.,[2] while a brief overview is given below. The Maxwell's equations that the solver employs are written in the frequency domain

$$\bigtriangledown \times \mathbf{E} = i\omega\mathbf{B}, \ \frac{1}{\mu_0} \bigtriangledown \times \mathbf{B} = -i\omega\mathbf{D} + \mathbf{j_a}. \tag{1}$$

In the plasma region, the relation between **D** and **E** is in form of

$$\mathbf{D} = \varepsilon_0(\varepsilon\mathbf{E} + ig[\mathbf{E}\times\mathbf{b}] + (\eta - \varepsilon)(\mathbf{E}\cdot\mathbf{b})\mathbf{b}), \tag{2}$$

where $\mathbf{b} \equiv \mathbf{B_0}/B_0$ is the unit vector along the static magnetic field and

$$\varepsilon = 1 - \sum_\alpha \frac{\omega + i\nu_\alpha}{\omega} \frac{\omega_{p\alpha}^2}{(\omega + i\nu_\alpha)^2 - \omega_{c\alpha}^2}, g = -\sum_\alpha \frac{\omega_{c\alpha}}{\omega} \frac{\omega_{p\alpha}^2}{(\omega + i\nu_\alpha)^2 - \omega_{c\alpha}^2}, \eta = 1 - \sum_\alpha \frac{\omega_{p\alpha}^2}{\omega(\omega + i\nu_\alpha)}. \tag{3}$$

Here the subscript α labels particle species, i. e. electron and ion, $\omega_{p\alpha} \equiv \sqrt{n_\alpha q_\alpha^2/\varepsilon_0 m_\alpha}$ is the plasma frequency, $\omega_{c\alpha} \equiv q_\alpha B_0/m_\alpha$ gyrofrequency, and ν_α collision frequency between species. The externally applied $B_0(r,\theta,z)$ is assumed to be axisymmetric, with $B_{0r} \ll B_{0z}$ and $B_{0\theta} = 0$. Therefore, it is appropriate to use a near axis expansion for $B_0(r,\theta,z)$,

$$B_{0r}(r,\ z) = -\frac{1}{2} r \frac{\partial B_{0z}(z)}{\partial z}. \tag{4}$$

We assume that the antenna current is divergence free, to eliminate the capacitive coupling. Fourier components of the antenna current density are given by

$$j_{ar} = 0, \tag{5}$$

$$\begin{aligned} j_{a\theta} = \quad & I_a \frac{e^{im\pi}-1}{2} \delta(r-R_a)\left(\frac{i}{m\pi}[\delta(z-z_a)+\delta(z-z_a-L_a)]\right. \\ & \left. + \frac{H(z-z_a)H(z_a+L_a-z)}{L_a} e^{-im\pi[1+(z-z_a)/L_a]}\right), \end{aligned} \tag{6}$$

$$j_{az} = I_a \frac{e^{-im\pi[1+(z-z_a)/L_a]}}{\pi R_a} \frac{1-e^{im\pi}}{2} \delta(r-R_a) \times H(z-z_a)H(z_a+L_a-z), \tag{7}$$

where L_a is the antenna length, R_a the antenna radius, z_a the distance between the antenna and the endplate in the source region, and H the Heaviside step function.

Boundary conditions

The radial wall of the target chamber and the axial endplates are ideally conducting so that the tangential components of $\mathbf{E}$ vanish at the surface of these boundaries,

$$E_\theta(L_r, z) = E_z(L_r, z) = 0, E_r(r, 0) = E_\theta(r, 0) = 0, E_r(r, L_z) = E_\theta(r, L_z) = 0, \tag{8}$$

where L_r and L_z are the radius of the target chamber and the length of the whole machine, respectively. Moreover, all field components must be regular on axis, thus, $B_\theta|_{r=0} = 0$ and $(rE_\theta)|_{r=0} = 0$ for $m = 0$; $E_z|_{r=0}$ and $(rE_\theta)|_{r=0}$ for $m \neq 0$.

Computed and measured wave fields

The RF field solver solves Eq. (1)-(2) for $\mathbf{E}$ based on given antenna current $\mathbf{j_a}$ and boundary conditions. Figure 3 shows the axial profiles of the computed B_r amplitude and phase on axis, and their comparisons with experimental data. A qualitative match between measurement and simulation of the axial variation of B_r is found using an enhancement in collisionality of $\nu_{\text{eff}} = \zeta(\nu_{ei} + \nu_{ie}) \approx \zeta \nu_{ei}$ with $\zeta = 9.5$, and an adjustment in antenna dimension of $R_{\text{sim}} = \xi R_{\text{exp}}$ with $\xi = 0.88$. Calculation of the axial gradient of the computed phase variation shows a travelling wave, with a good agreement with data.

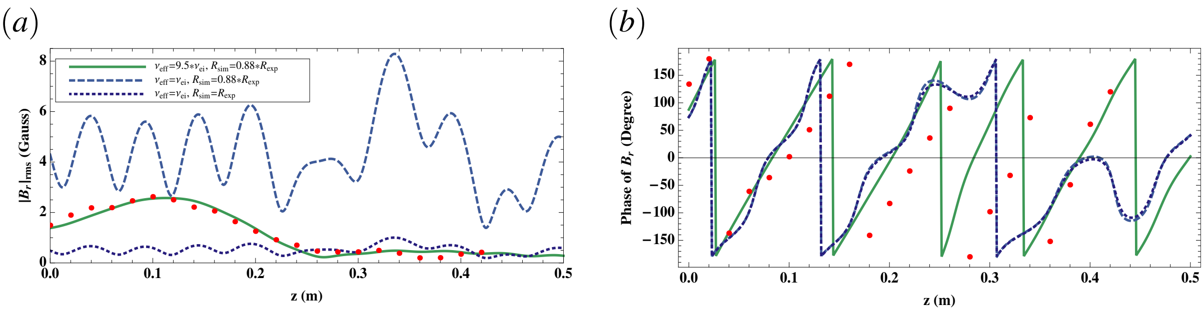

Figure 3: Variations of magnetic wave field in axial direction (on-axis): (a) $|B_r|_{\text{rms}}$, (b) phase of B_r. Computed results (lines) are compared with experimental data (dots).

Figure 4 shows the radial profiles of computed wave fields for $\nu_{\text{eff}} = 9.5\nu_{ei}$ and $R_{\text{sim}} = 0.88R_{\text{exp}}$ at three axial positions in the target region, together with the experimental data measured at $z = 0.17$ m. Inspection of Fig. 4 reveals that it is possible to find a reasonable agreement to the wave amplitude and phase profile, albeit independently.

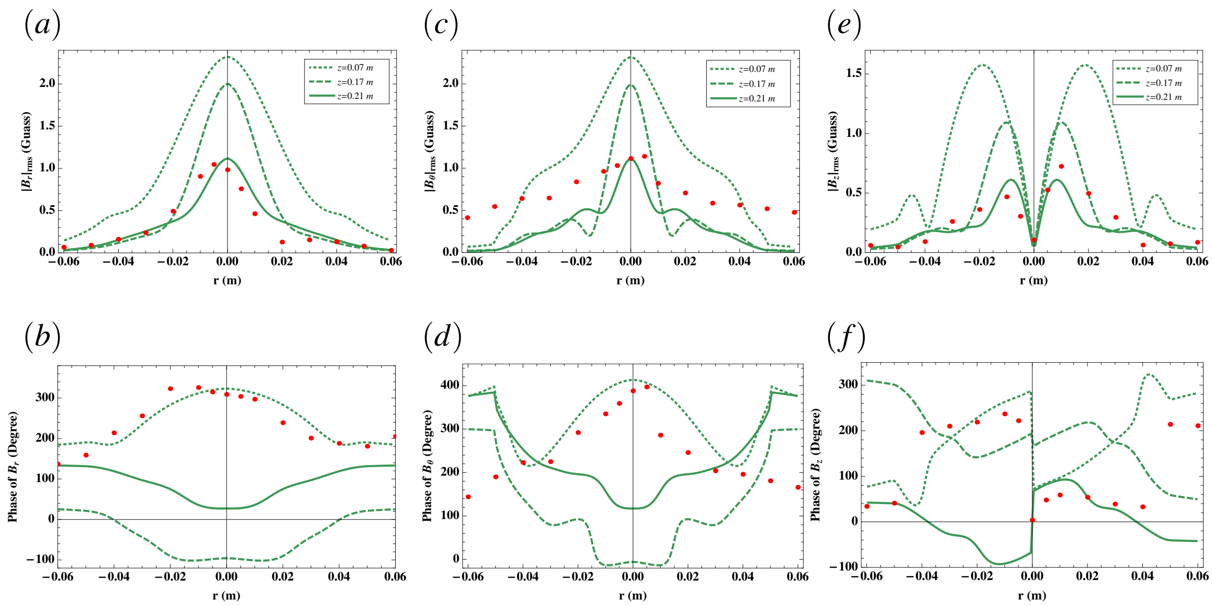

Figure 4: Variations of magnetic wave field in radial direction: (a), (c) and (e) are $|B_r|_{\text{rms}}$, $|B_\theta|_{\text{rms}}$ and $|B_z|_{\text{rms}}$, respectively; (b), (d) and (f) are the corresponding phase variations. Dots are experimental data.

Conclusion

With an enhancement factor of 9.5 to the electron-ion Coulomb collision frequency, 12% reduction in the antenna radius, and the same other conditions as employed in the experiment, the solver produces axial and radial profiles of wave amplitude and phase that are consistent with measurements.

Acknowledgement

Lei Chang appreciates the financial support provided by Chinese Scholarship Council for his PhD study at the Australian National University, and the Student Conference Support from Australian Institute of Physics for him to present this work in 39th European Physical Society Conference on Plasma Physics and 16th International Congress on Plasma Physics.

References

[1] B. D. Blackwell, J. F. Caneses, C. Samuell, J. Wach, J. Howard, and C. S. Corr, submitted on 25 March 2012 to Plasma Sources Science and Technology.

[2] G. Chen, A. V. Arefiev, R. D. Bengtson, B. N. Breizman, C. A. Lee, L. L. Raja, Phys. Plasmas, **13**, 123507, (2006)